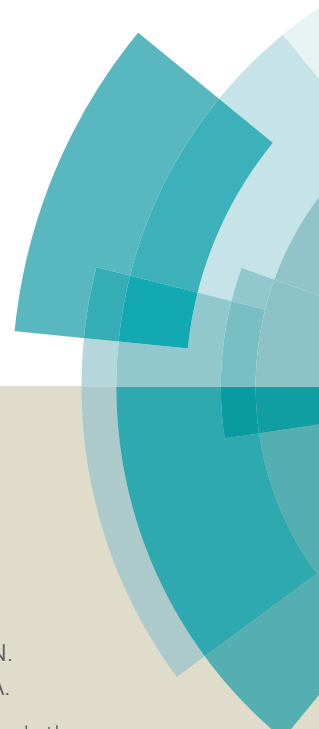


PCCP

Accepted Manuscript



This article can be cited before page numbers have been issued, to do this please use: C. Obondi, G. N. Lim, P. A. Karr, V. Nesterov and F. DSouza, *Phys. Chem. Chem. Phys.*, 2016, DOI: 10.1039/C6CP03479A.



This is an *Accepted Manuscript*, which has been through the Royal Society of Chemistry peer review process and has been accepted for publication.

Accepted Manuscripts are published online shortly after acceptance, before technical editing, formatting and proof reading. Using this free service, authors can make their results available to the community, in citable form, before we publish the edited article. We will replace this *Accepted Manuscript* with the edited and formatted *Advance Article* as soon as it is available.

You can find more information about *Accepted Manuscripts* in the [Information for Authors](#).

Please note that technical editing may introduce minor changes to the text and/or graphics, which may alter content. The journal's standard [Terms & Conditions](#) and the [Ethical guidelines](#) still apply. In no event shall the Royal Society of Chemistry be held responsible for any errors or omissions in this *Accepted Manuscript* or any consequences arising from the use of any information it contains.

Photoinduced charge separation in wide-band capturing, multi-modular bis(donor styryl)BODIPY-fullerene systems

Christopher O. Obondi,^a Gary N. Lim,^a Paul A. Karr,^b Vladimir N. Nesterov,^a
and Francis D'Souza^{a,*}

^aDepartment of Chemistry, University of North Texas, 1155 Union Circle, #305070, Denton, TX
76203-5017, USA; E-mail: Francis.DSouza@UNT.edu;

^bDepartment of Physical Sciences and Mathematics, Wayne State College, 111 Main Street,
Wayne, Nebraska 68787, USA

(Abstract) A new series of multi-modular donor-acceptor systems capable of exhibiting photoinduced charge separation have been designed, synthesized and characterized using various techniques. In this series, the electron donor was a BF₂-chelated dipyrromethene (BODIPY) appended with two styryl linkers carrying two electron rich triphenylamine or phenothiazine entities. Fulleropyrrolidine linked at the *meso*-position of the BODIPY ring served as an electron acceptor. As a result of extended conjugation and multiple electroactive chromophore entities, the bis-styryl BODIPY revealed absorbance and emission well-into the near-infrared region covering 300-850 nm spectral range. Using redox, computational, absorbance and emission data, an energy level diagram was constructed that helped in envisioning the different photochemical events. Spectral evidence for photoinduced charge separation in these systems was established from femtosecond and nanosecond transient absorption studies. The measured rate constants indicated fast charge separation and relatively slow charge recombination revealing their usefulness in light energy harvesting and optoelectronic device building applications. The bis(donor styryl)BODIPY-fullerene systems populated BODIPY triplet excited states during the process of charge recombination.

1. Introduction

Photoactive multi-modular donor-acceptor systems capable of mimicking the primary events of natural photosynthesis is one of the active research areas in modern chemical science.¹⁻¹⁸ Towards this, a number of donor-acceptor systems have been constructed and formation of charge separated states upon photoexcitation of either the donor or acceptor entity have been demonstrated. Among the organic photosensitizers, porphyrins and phthalocyanines are the widely used class of compounds while the role of electron acceptor has been mainly fulfilled by fullerene, C₆₀.¹⁻¹⁸ Wealth of information, largely on the structure-spectral, structure-redox, and structure-photochemical properties of the donor-acceptor systems have been gathered from these studies. Systems that performed well have eventually been used in the construction of light-to-electricity and light-to-fuel conversion devices.¹⁹

In recent years, utilization of BODIPYs (= BF₂-cheated dipyrromethene, derived from 4,4-difluoro-1,3,5,7-tetra-methyl-4-bora-3a,4a diaza-s-indacene) and azaBODIPYs (= BF₂-cheated azadipyrromethene) in the construction of donor-acceptor conjugates have gained appreciable momentum.¹⁰ Both are stable compounds allowing one to perform a wide range of reactions to tune their spectral, electrochemical and photochemical properties, needed in building novel donor-acceptor architectures. Depending upon the counter molecular entity, these compounds can fulfill the role of either an energy/electron donor or acceptor. Other applications of BODIPYs and azaBODIPYs include their utilization in developing chemosensors and imaging agents for biochemical applications.²⁰

In the present study, we have designed and synthesized a supramolecular conjugate comprised of BODIPY and fullerene (**1** in Fig. 1). Further, in order to capture light beyond 525 nm of pristine BODIPY absorption, the BODIPY in the dyad has been π -extended to possess two styryl groups shown as **2** in Fig. 1.²¹ Additionally, to build multi-modular donor-acceptor assemblies, the styryl groups of BODIPY have been terminated with secondary electron donors viz., triphenylamine (**3**) and phenothiazine (**4**).²² The structures of these molecules are shown in Fig. 1. Upon characterization of these conjugates using spectral, electrochemical and computational methods, photoinduced charge separation has been systematically investigated using femtosecond and nanosecond transient spectroscopic techniques.

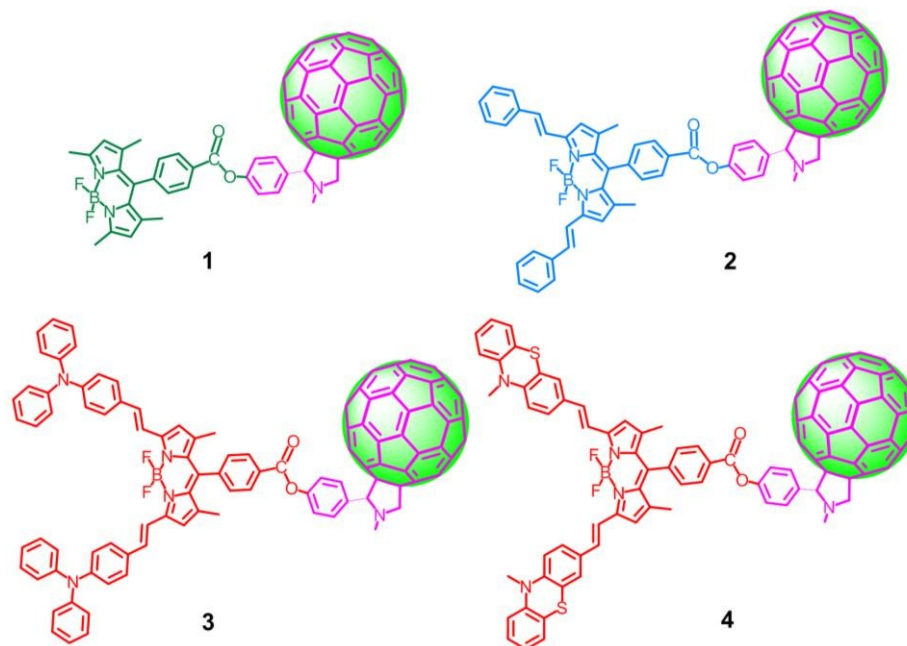


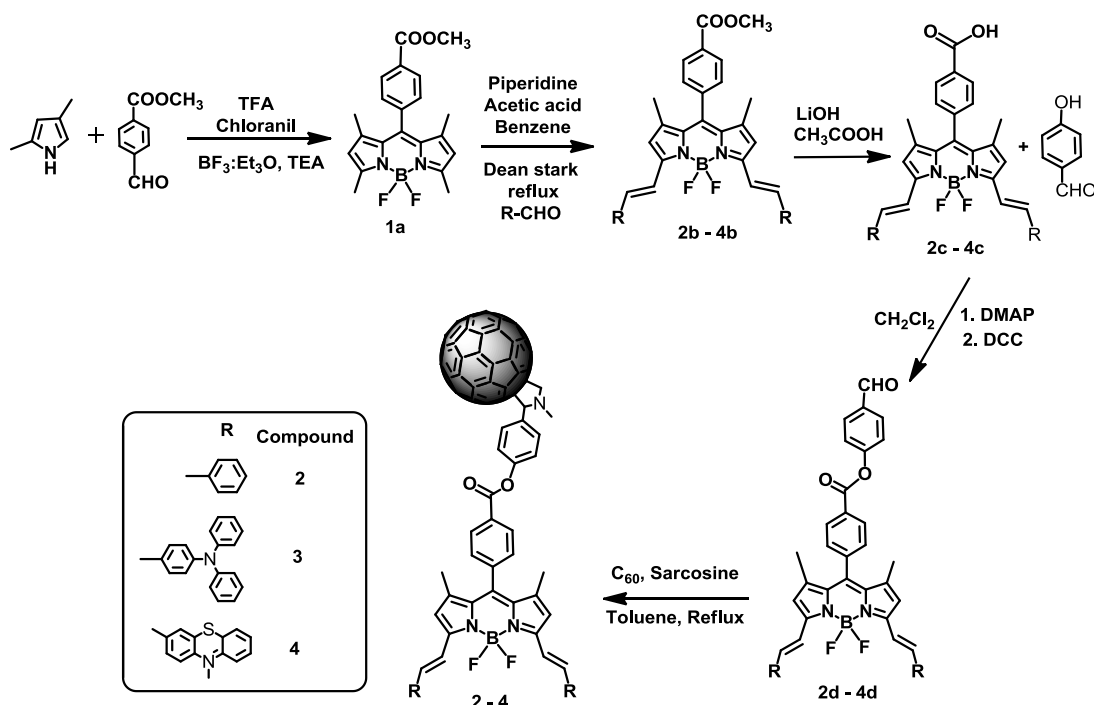
Fig. 1. Structure of the BODIPY- C_{60} (**1**), bis(phenyl styryl)BODIPY- C_{60} (**2**), bis(triphenylamine styryl)BODIPY- C_{60} (**3**), and bis(phenothiazine styryl)BODIPY- C_{60} (**4**) multi-modular systems developed to probe photoinduced electron transfer.

2. Results and Discussion

2.1 Synthesis and X-ray structure of bis(styryl)BODIPY

The synthesis of the multi-modular donor-acceptor systems was accomplished by a multi-step synthetic procedure as outlined in Scheme 1. Briefly, 2,4-dimethyl pyrrole was reacted with methyl 4-formylbenzoate in dry dichloromethane and trifluoroacetic acid followed by p-chloranil reaction and treatment with boron trifluoroborane etherate in triethylamine. The desired compound **1a** was purified over silica gel column. For syntheses of compounds **2b-4b**, compound **1a** was used as the starting material and was treated with benzaldehyde (for **2b**), or 4-(diphenylamino)benzaldehyde (for **3b**) or 3-formyl-10-methyl phenothiazine (for **4b**) in dry benzene using Dean-Stark apparatus to separate water from the reaction mixture. Next, compounds **2b-4b** were hydrolyzed using LiOH in acetic acid to obtain **2c-4c** that was followed by reacting them with 4-hydroxybenzaldehyde to obtain compounds **2d-4d**. Finally, **2d-4d** were reacted with C_{60} and sacosine in toluene to obtain the final multi-modular products, **2-4**. For compound **1**, the step involving styryl groups attachment was avoided and rest of the steps were

followed. The final compounds were purified by column chromatography and purity was checked by thin-layer chromatography. The structural integrity was established from ^1H and ^{13}C NMR, MALDI-TOF-mass, spectral and electrochemical studies. Synthesis of control compounds, **5-8** (see Fig. S1 for structures) were carried out according Scheme S1 in ESI. The compounds were stored in dark prior performing spectral and transient absorption measurements.



Scheme 1. Synthetic methodology adopted for bis(donor styryl)BODIPY- C_{60} multi-modular donor-acceptor systems.

The X-ray structure and packing diagram of bis(phenyl styryl)BODIPY, **6** is shown in Fig. 2a (see Scheme S1 in the ESI for structure). The molecule crystallized in the triclinic crystal system with space group P-1.²³ The boron of BODIPY macrocycle assumed a tetrahedral geometry with the two ring nitrogens and two fluorines. In agreement with previous structural reports on BODIPYs,²⁴ the core of the BODIPY macrocycle was flat while the *meso*-phenyl ring was almost orthogonal with a torsion angle of 76° . The phenyl ring attached to the styryl groups were slightly tilted with torsion angles of 23.7° and 29.8° , respectively, and were spatially separated by over 8.0 \AA causing no steric hindrance. The crystal packing diagram shown in Fig. 2b revealed

no significant intermolecular interactions. The atomic coordinates, bond lengths and angles, anisotropic displacement parameters, hydrogen coordinates (Tables S1-S5) are given in the ESI.

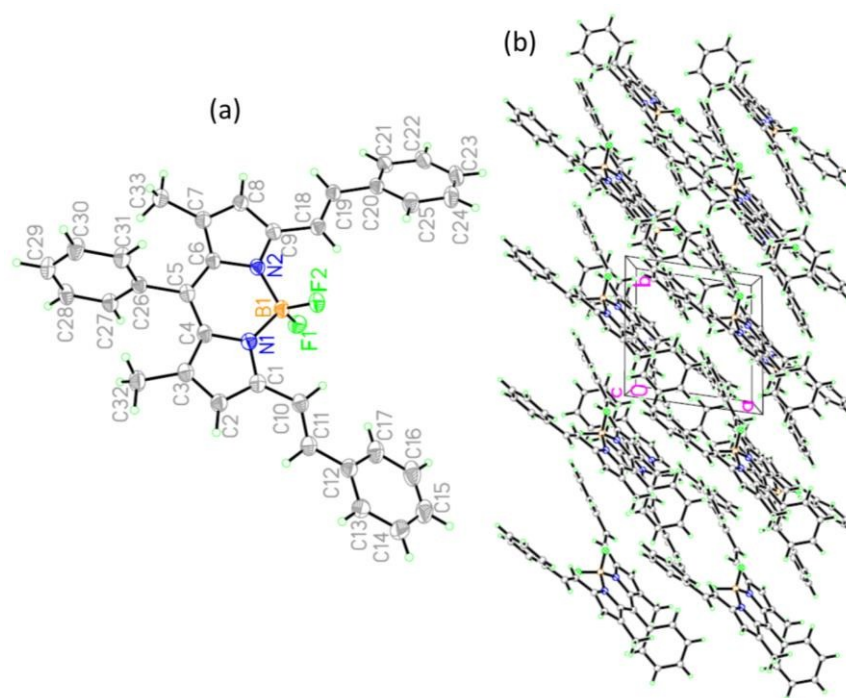


Fig. 2. Projection and crystal packing diagrams of bis(styryl)BODIPY with 50% thermal ellipsoids.

2.2 Absorbance and fluorescence studies

Normalized absorption spectra of the investigated donor-acceptor systems is shown in Fig. 3 while Fig. S2 in ESI shows the spectra of the control compounds, viz., the BODIPY derivatives lacking electron acceptor, C₆₀ (compounds **5-8**). The two styryl entities in the case of **2** and **6** caused bathochromic shift of the absorption bands by about 125 nm compared with pristine BODIPY, **1** or **5**. That is, the 505 nm peak observed in the case of **1** and **5** appeared at 634 and 628 nm, respectively, for **2** and **6** primarily due to extended conjugation effect of the two styryl tails. Appending C₆₀ caused an additional 6 nm red-shift in the case of **2** as compared with **6**. In all of the donor-acceptor conjugates, **1-4**, a characteristic sharp peak of fulleropyrrolidine at 432 nm was also observed. Interestingly, in the case of **3** and **4**, and their respective control compounds **7** and **8** having either two triphenylamine or phenothiazine entities, additional bathochromic shifts were noticed. In the case of **3** the main peak was at 676 while for **4** this peak was at 702 nm. For control **7** the main peak was at 685 nm and for **8** this

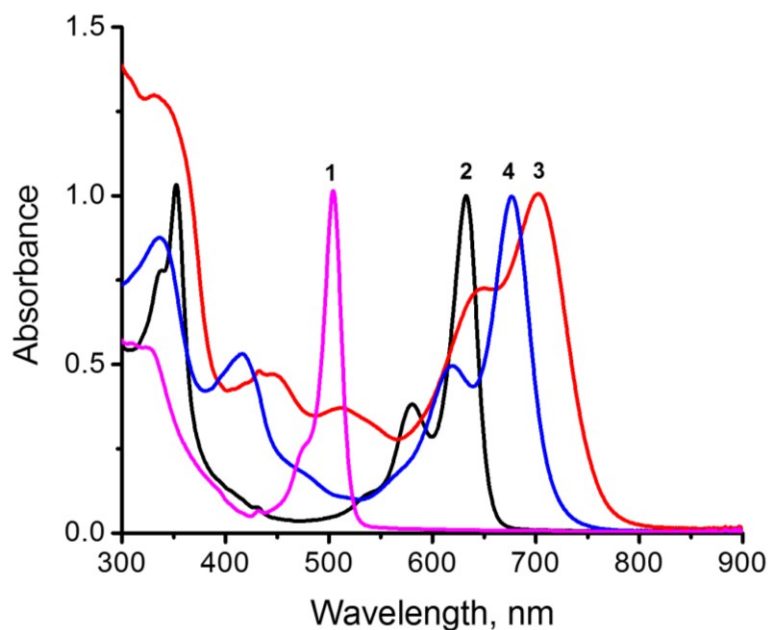


Fig. 3. Absorption spectra (normalized to the most intense peak maxima) of the indicated compounds in benzonitrile.

Table 1. Absorption, fluorescence and singlet excited state lifetime data of the investigated compounds.

Compound ^a	Absorption peak maxima, λ nm	Fluorescence peak maxima, λ nm	Fluorescence quantum yield, Φ_f	Lifetime, ns
1	313, 506	516	0.04	0.2
2	352, 581, 634	652	0.114	0.3
3	334, 418, 619, 676	763	0.07	1.0
4	330, 440, 509, 650, 702	709	<0.01	<0.1
5	314, 505	516	0.577	3.33
6	578, 628	641, 699(sh)	0.571	3.74
7	445, 685	754, 820(sh)	0.203	2.73
8	636, 696	708	<0.01	0.05

^a-see Fig. 1 and Fig. S1 for structures

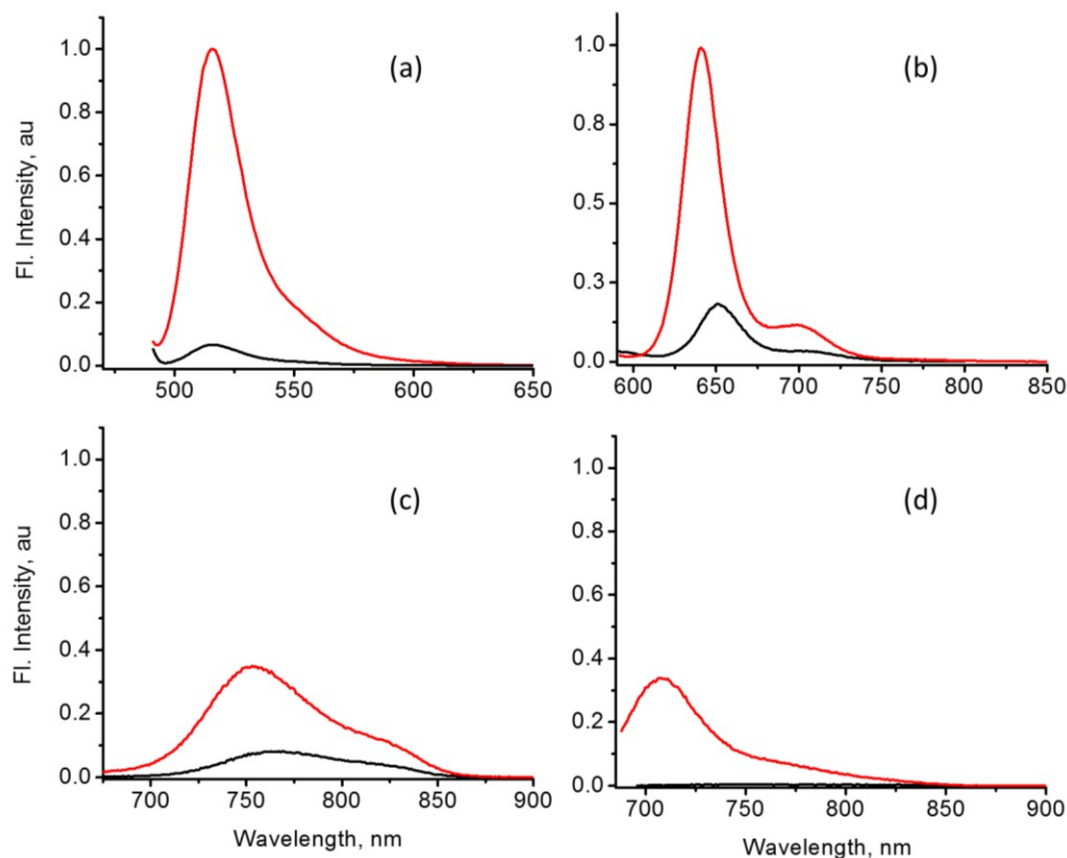


Fig. 4. Fluorescence spectra of (a) **1** (black) and **5** (red), (b) **2** (black) and **6** (red), (c) **3** (black) and **7** (red), and (d) **4** (black) and **8** (red) in benzonitrile. The samples were excited at the most intense normalized peak maxima shown in Fig. 2.

was at 696 nm. These results indicate strong interactions between the triphenylamine or phenothiazine with the BODIPY via the styryl linkers.²² Table 1 lists the peak maxima for all the studied compounds. It is important to note that in the case of **3** and **4**, absorption peaks covering the entire 300-780 nm were observed, signifying the importance of the present approach towards wide-band capturing multi-modular systems.

Fig. 4 displays the fluorescence spectra of the investigated donor-acceptor systems along with their control compounds while the data are summarized in Table 1. Trends similar to that observed in the case of absorption spectra were observed. That is, bathochromically shifted peak maxima with significant degree of spectral broadening. Appending the triphenylamine and phenothiazine entities caused additional red-shift accompanied by diminished intensities. While

the fluorescence intensities of **5** and **6** were comparable, about 65% diminished intensity was observed for **7** and **8** due to the presence of triphenylamine and phenothiazine entities. These observations suggest that the triphenylamine and phenothiazine entities in **7** and **8** are involved in excited state events. Presence of C₆₀ in the donor-acceptor conjugates caused additional quenching. The percent quenching due to C₆₀ was 93%, 80%, 77% and 99%, respectively, for **1**, **2**, **3**, **4** as compared to their control compounds, **5-8**. Such quenching could mainly arise from either energy or electron transfer from the singlet excited BODIPY derivatives.²⁵ At this point, additional electrochemical and computational studies were warranted in search for an answer for the quenching mechanism.

2.3 Computational and electrochemical studies

Computational studies were performed to visualize the geometry and electronic structure of the supramolecular donor-acceptor assemblies. In these studies, the geometry of supramolecular structures **1-4** were optimized to a stationary point on the Born-Oppenheimer surface using the B3LYP method and the 6-31G(d,p) split valence basis set, to form the B3LYP/6-31G(d,p) model chemistry as parameterized in the *Gaussian-09* software.²⁶ The structures and orbitals (HOMO and LUMO) were visualized with the *GaussView* software. As shown in Fig. 5, in the optimized structures the HOMO was delocalized over the entire molecule including BODIPY, styryl tails and the donor entities while the LUMO was on C₆₀. These results suggest that the donor entities of **3** or **4** acting as a single entity, although some intramolecular push-pull type interactions between the entities could be envisioned from the location of the LUMO orbitals. Such charge transfer type interactions could be responsible for the reduced fluorescence as compared to that of **2**. The distance between the centers of fullerene to boron of BODIPY was found to be 18.37 Å in **1** and 18.28 Å in **2**, respectively. While the distances between the center of fullerene to the nitrogens of the triphenylamine entities in **3** were 26.27 Å and 25.39 Å. The distances between the center of fullerene to the nitrogens of the phenothiazine entities in **4** were found to be 26.46 Å and 23.83 Å. As pointed out earlier, no noticeable interactions between fullerene and BODIPY π -structure were observed in any one of the conjugates.

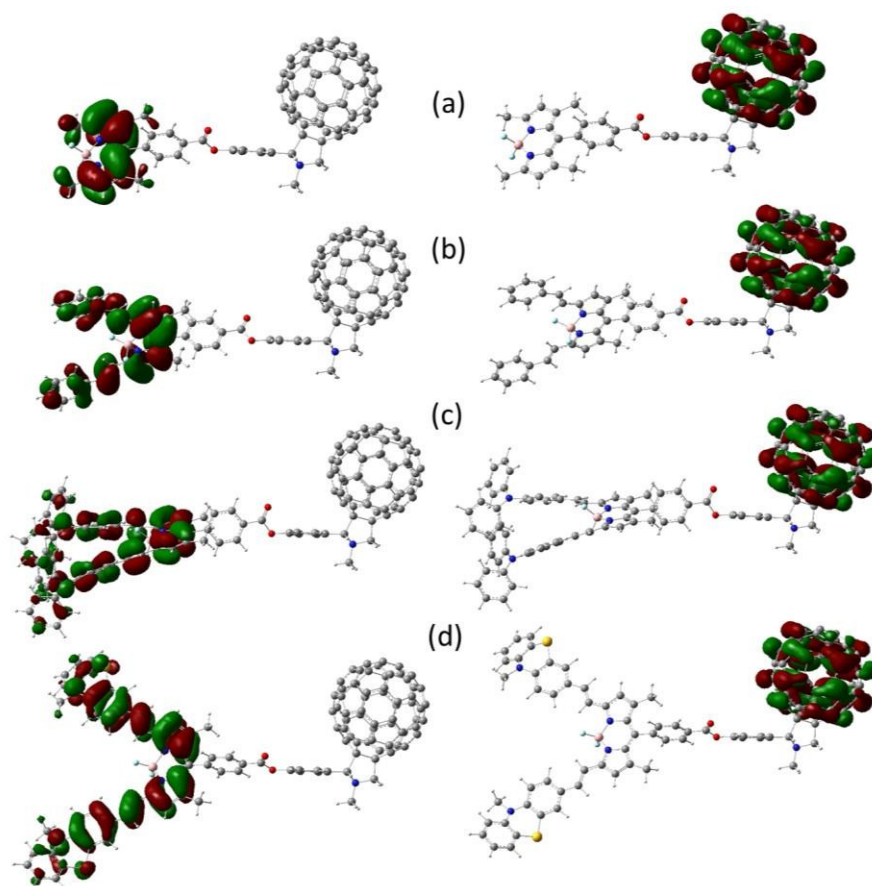


Fig. 5. Frontier HOMO (left) and LUMO (right) of (a) **1**, (b) **2**, (c) **3**, and (d) **4** generated using *GaussView* on their respective B3LYP/6-31G** optimized structure.

Electrochemical studies using differential pulse (DPV) and cyclic voltammetry (CV) were performed to evaluate the redox potentials of compounds **1-8** and to calculate the energetics of the charge separation processes. Fig. 6 shows the DPV curves for compounds **1-4** in benzonitrile, 0.1 M (*n*-Bu₄N)ClO₄ while the CVs are shown in Fig. S4 in ESI. Multiple oxidation processes were observed. The redox potentials of the BODIPY segment in **1** were very similar to pristine BODIPY, **5**²⁷ while having two styryl groups in compound **2** affected both oxidation and reduction potentials. That is, lower oxidation and reduction potentials affecting the overall HOMO-LUMO gap was noticed (see potentials corresponding to first oxidation and second reduction in Table 2). Further, appending triphenylamine or phenothiazine entities had additional effect on the oxidation potentials compared to that over the reduction potentials. That is, lowered oxidation potential resulting in smaller HOMO-LUMO gap in the case of **3** and **4** compared to that in **2** was observed. In all these donor-acceptor systems, the first reduction

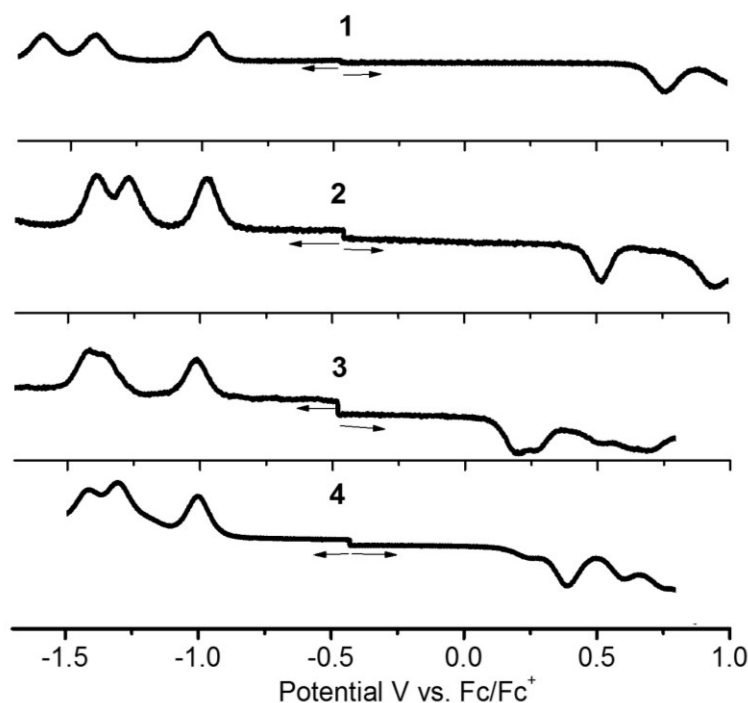


Fig. 6. Differential pulse voltammograms (DPVs) corresponding to both oxidation and reduction processes of the indicated compounds in benzonitrile containing 0.1 M (*t*-Bu₄N)ClO₄ as supporting electrolyte. Scan rate = 5 mV/s, pulse width = 0.25 s, pulse height = 0.025 V.

Table 2. Redox potentials, free-energy change for charge separation (ΔG_{CS}) and recombination (ΔG_{CR}) for the donor-acceptor conjugates in benzonitrile.

Compound	1 st Ox ^a	1 st Red ^b	2 nd Red ^c	$-\Delta G_{CR}$, eV ^e	$-\Delta G_{CS}$, eV ^e
1	0.76	-1.01	-1.59 ^d	1.72	0.71
2	0.52	-1.00	-1.27	1.46	0.48
3	0.20	-1.01	-1.36	1.16	0.57
4	0.39	-1.00	-1.31	1.32	0.43

^a-bis(donor styryl)BODIPY centered

^b-C₆₀ centered

^c- bis(donor styryl)BODIPY centered

^d-third reduction wave

^e-see text for relevant equations

potential corresponding to C₆₀ revealed no significant changes meaning absence of significant intramolecular interactions with the BODIPY π -system, as predicted by computational studies.

Table 2 lists the first oxidation and first two reduction potentials needed to calculate the free-energy changes of these investigated compounds.

The free energy change for charge separation (ΔG_{CS}) from the singlet excited state of the modified BODIPY within the donor-acceptor system was calculated using spectroscopic, computational and electrochemical data following equations 1-3.²⁸

$$-\Delta G_{CR} = E_{ox} - E_{red} + \Delta G_s \quad (1)$$

$$-\Delta G_{CS} = \Delta E_{00} - (-\Delta G_{CR}) \quad (2)$$

where ΔE_{00} and ΔG_{CS} correspond to the energy of excited singlet state being, 2.43 eV for **1**, 1.94 eV for **2**, 1.73 eV for **3**, and 1.75 eV for **4**,²² and electrostatic energy, respectively. The E_{ox} and E_{red} represent the oxidation potential of the electron donor (BODIPY) and the reduction potential of the electron acceptor (C_{60}), respectively. The term ΔG_s refers to the static Coulombic energy, calculated by using the “dielectric continuum model” according to equation (3):

$$\Delta G_s = \frac{e^2}{4\pi\epsilon_0} \left[\left(\frac{1}{2R_+} + \frac{1}{2R_-} \right) \Delta \left(\frac{1}{\epsilon_R} \right) - \frac{1}{R_{CC}\epsilon_R} \right] \quad (3)$$

The symbols ϵ_0 , and ϵ_R represent vacuum permittivity and dielectric constant of the solvent used for photochemical and electrochemical studies, respectively. R_{CC} is the center-to-center distance between donor and acceptor entities. The symbols R_+ and R_- refer to radii of the cation and anion species, respectively. The calculated ΔG_s was found to be 0.07 ± 0.02 eV for the present donor-acceptor systems.

Fig. 7 shows an energy level diagram constructed using spectral and free energy calculations data depicting different photophysical events in the donor-acceptor systems. In all of these dyads, formation of $D^{+}C_{60}^{-}$ charge separated state from ${}^1D^*$ (where D = BODIPYs) is evident. Singlet-singlet energy transfer from ${}^1D^*$ to C_{60} to produce ${}^1C_{60}^*$ is also possible. Formation of $D^{+}C_{60}^{-}$ from ${}^1C_{60}^*$ is also a possibility, however, at the excitation wavelength of 400 nm, most of the light was absorbed by the BODIPY sensitizers, hence this could be considered to be a minor process. Once formed, the $D^{+}C_{60}^{-}$ charge separated state could relax directly to the ground state or alternatively populate the triplet excited state of either BODIPY or fullerene entities. Energetically, charge separated state formed by **1** (energy level shown in blue) could populate either ${}^3BODIPY^*$ or ${}^3C_{60}^*$ states, while for radical ion-pairs involving conjugates

2-4, population of only $^3\text{BODIPY}^*$ is energetically possible. In order to unravel these mechanistic routes and to secure evidence for charge separation, transient absorption studies using femtosecond and nanosecond transient techniques were systematically performed and the outcome of these results are discussed below.

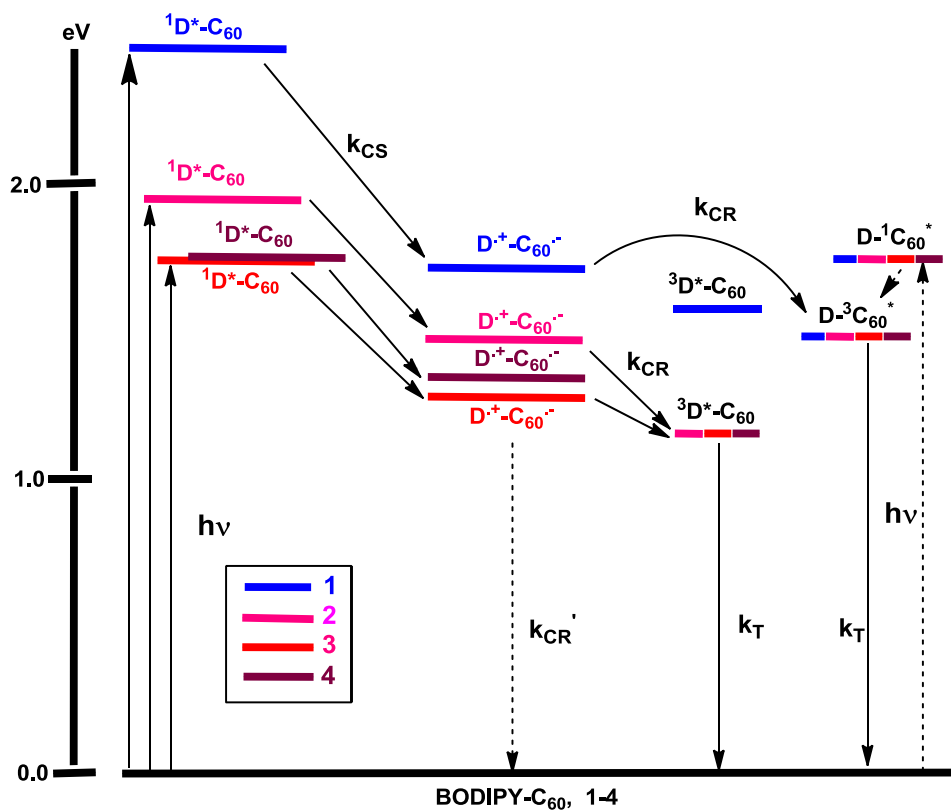


Fig. 7. Energy level diagram showing the different photochemical events in donor-acceptor conjugates, **1-4** in benzonitrile. Energies of different states were evaluated from spectral and electrochemical studies. Energy of $^3[\text{bis}(\text{styryl})\text{BODIPY}]^*$ was taken from Ref. 21a. Solid arrow indicates major photo processes, dashed arrow indicates minor photo processes. Abbreviations: CS = charge separation, CR = charge recombination, EnT = energy transfer, T = triplet state.

2.4 Femtosecond and nanosecond transient absorption studies

To aid-in spectral interpretation, the one-electron oxidation products of compounds **5-8** by chemical oxidation using nitrosonium hexafluoroborate as an oxidizing agent in benzonitrile were carried out, and spectral data is shown in Fig. S3. For **5**, during oxidation, a new peak at 497 nm close to the intense peak of the neutral compound at 505 nm was observed (Fig. S3a). For compounds **6-8** with two π -extended styryl chains, the spectral identity of radical cation peaks was distinct from the peaks of the neutral compound. As shown in Fig. S3b, for **6**, new

peaks at 529 and 567 nm corresponding to [bis(phenyl styryl)BODIPY]⁺ (**6**⁺) was observed. For **7**, peaks at 520 and 601 nm, and for **8** peaks at 466, and 625 nm, corresponding to their respective radical cation were observed (Fig. S3c and 3d). Peaks corresponding to C₆₀^{•+} at 1020 nm for fulleropyrrolidine derivatives is well-known.⁷ Presence of transient absorption bands at these locations would provide evidence of charge separation in these dyads.

Next, femtosecond transient spectra of the functionalized BODIPY derivatives **6-8** along with pristine BODIPY, **5** was investigated in benzonitrile. For the large part, spectral features were similar to the earlier reported on crown ether appended BODIPY derivatives.²² As shown in Fig. 8a for compound **5**, the instantaneously formed singlet BODIPY revealed a negative peak at 508 nm having contributions from ground state absorption and stimulated emission of

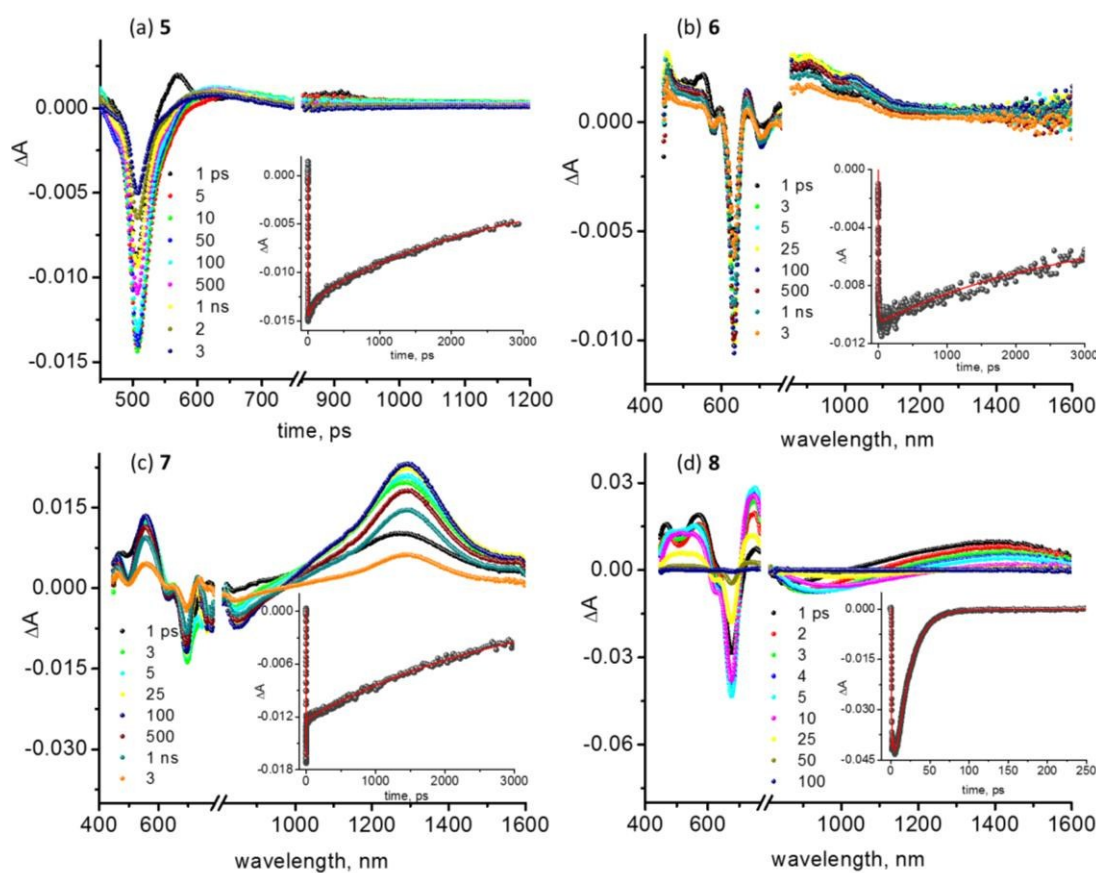


Fig. 8. Femtosecond transient spectra (100 fs pulse width at 400 nm) of the indicated compounds in Ar-saturated benzonitrile at the indicated delay times. The time profiles of the peak corresponding to ground state bleaching are shown as figure insets.

BODIPY. Recovery of the 508 nm peak (Fig. 8a inset) was slow as predicted by its relatively long fluorescence lifetime (Table 1). The transient spectral features of bis(phenyl styryl)BODIPY in benzonitrile is shown in Fig. 8b. Positive peaks at 544, 594, 667, 830, 944 and 1016 nm, and negative peaks at 576, 631 and 704 nm were observed. The positive peaks are mainly attributed to the instantaneously formed singlet excited state transitions. The first two negative peaks corresponded mainly to the ground state bleaching as the absorption peak maxima matched well with these peaks while the 704 nm peak was due to stimulated emission of the styryl BODIPY entity. Recovery of the 634 nm peak is shown in Fig. 8b inset where relatively slow recovery was observed.

The femtosecond transient spectral features of compounds **7** and **8** having triphenylamine and phenothiazine, respectively, were considerably different from that observed for compounds **5** and **6** due to the interactions of these entities with the bis-styryl BODIPY π -system.²² Compound **7** revealed positive peaks at 458, 556, 649, 732, and 1292 nm and negative peaks at 631, 694 and 852 nm (Fig. 8c). The negative peaks corresponded to the ground state bleaching and stimulated emission. Time constant for the recovery of the 694 nm peak was about 3180 ps (Fig. 8b inset). The broad near-IR peak is attributed to the singlet-singlet transition of the singlet excited **7**. The reduced fluorescence lifetime and quantum yield of **7** compared to either **5** and **6** is supportive of intramolecular charge transfer type interactions involving the triphenylamine entities. The spectral features observed for **8** having two phenothiazine entities linked to the bis-styryl BODIPY unit were comparatively short lived (Fig. 8d). Positive peaks at 467, 570, 751, and 1400 nm and negative signal at 675 nm were observed. The strong negative peak at 675 nm corresponding to ground state bleaching revealed faster recovery (Fig. 8d inset), in agreement with its lower fluorescence lifetime. However, no strong negative signal in the 720 nm region revealing for stimulated emission was observed supporting occurrence of rapid intramolecular events. Similar to compound **7**, the near-IR peak at 1400 nm of **8** revealed initial growth followed by rapid decay. The time constants for growth and decay of this signal was found to be 14.9 and 105.5 ps, respectively, revealing occurrence of rapid intramolecular charge transfer type interactions involving the phenothiazine and styryl BODIPY entities.

Fig. 9a shows the femtosecond transient spectra at different delay times of **1** in benzonitrile. Evidence for charge separation from the ¹BODIPY* was evident from the spectral observations.

That is, a transient peak at 500 nm range corresponding to BODIPY⁺⁺ and a near-IR band at 1020 nm characteristic of C₆₀^{•-} was obtained. Note the weak BODIPY⁺⁺ peak in the 500 nm range developing at the latter time scale due to the presence of strong negative peak at 506 nm corresponding to ground state depletion and stimulated emission of ¹BODIPY*. The recovery of the 506 nm peak was faster than that observed in pristine **5**, due to additional charge separation process. The rate constant of charge separation, *k*_{CS} and charge recombination, *k*_{CR}, evaluated by monitoring rise and decay of the C₆₀^{•-} (see Fig. 9a inset for decay time profile) and were found to be 1.8 × 10¹⁰ s⁻¹ and 7.5 × 10⁸ s⁻¹, respectively. Faster charge separation and relatively slow charge recombination were observed. The decay of the C₆₀^{•-} peak representing charge recombination was accompanied by a new peak in the 700 nm range corresponding to the

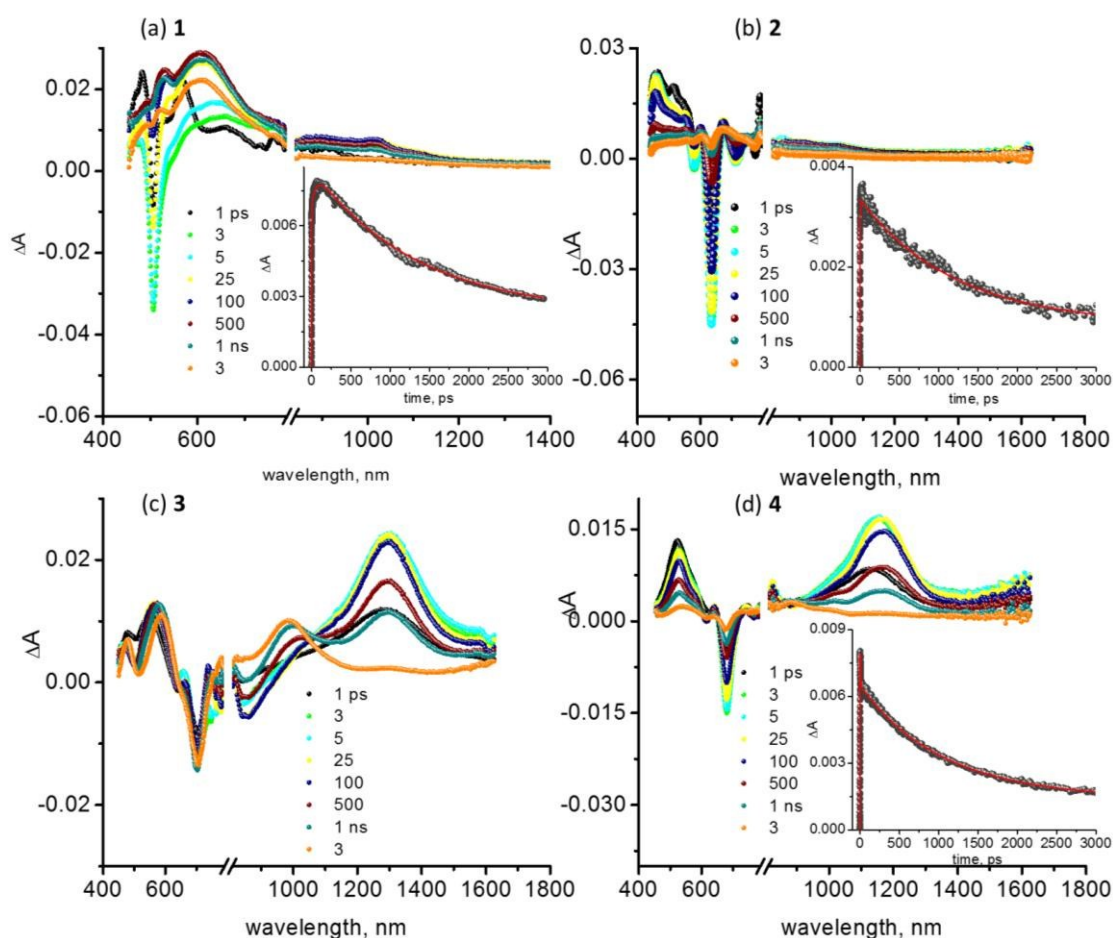


Fig. 9. Femtosecond transient spectra (100 fs pulse width at 400 nm) of the indicated compounds in Ar-saturated benzonitrile at the indicated delay times. The time profiles of the peak corresponding to C₆₀^{•-} monitored at 1020 nm is shown in figure inset.

formation of ${}^3\text{C}_{60}^*$. These results indicate that the charge separated state populates the ${}^3\text{C}_{60}^*$ prior returning to the ground state.

Femtosecond transient absorption spectra of **2** in benzonitrile is shown in Fig. 9b. The decay of peaks corresponding to singlet excited state and recovery of the 636 nm peak were much faster than that observed for control compound **6** lacking the C_{60} entity. This was accompanied by new peaks in the 570 corresponding to the formation of BODIPY^{++} and 1020 nm range corresponding to $\text{C}_{60}^{\bullet-}$. The k_{CS} and k_{CR} evaluated by monitoring rise and decay of the $\text{C}_{60}^{\bullet-}$ (see Fig. 9b inset) were found to be $2.2 \times 10^{11} \text{ s}^{-1}$ and $8.2 \times 10^8 \text{ s}^{-1}$, respectively. Femtosecond transient spectra corresponding to **3** and **4** were much more complex to establish charge separation due to intense transient peaks of triphenylamine and phenothiazine appended styryl BODIPYs as shown in Fig. 9c and 9d. In the case of **3**, the radical cation peak appeared as a shoulder peak at 610 nm to the main peak at 560 nm while the radical anion peak appeared as a shoulder at peak 1020 nm to the main peak at 1300 nm. Fig. 10a shows spectrum at 50 ps for **3** and the control compound **7** that clearly shows transient peaks of the radical ion-pair demonstrating occurrence of charge separation in **3**. The strong overlap of the radical ion-pair and the broad singlet excited state of bis(triphenylamine styryl)BODIPY at 1295 nm made almost impossible to evaluate the k_{CS} and k_{CR} from the radical-ion pair. Hence, it was then evaluated from the changes in the kinetics of the singlet excited state at 1295 nm. The estimated k_{CS} and k_{CR} were $3.1 \times 10^{11} \text{ s}^{-1}$ and $2.3 \times 10^8 \text{ s}^{-1}$, respectively. A similar case was also observed

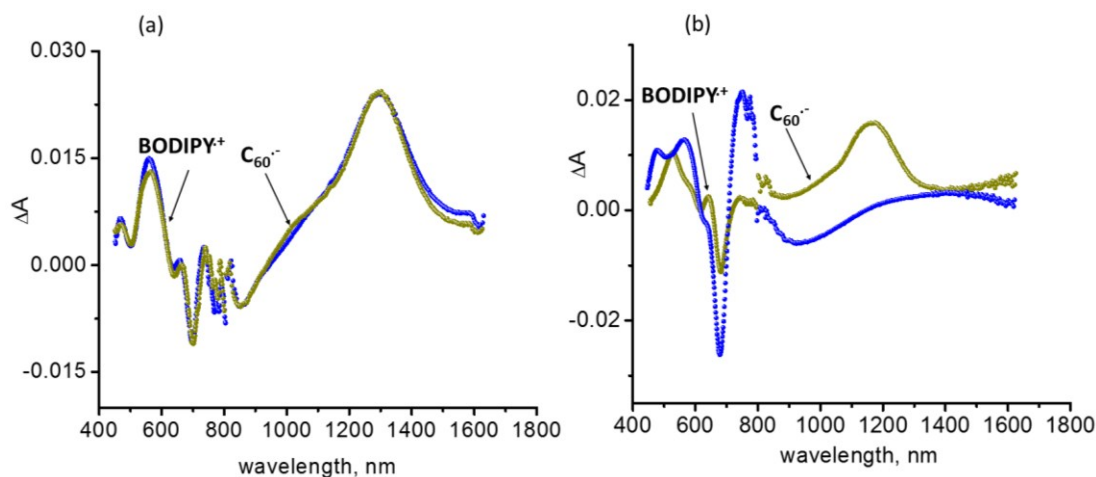


Fig. 10. Femtosecond transient spectrum (100 fs pulse width at 400 nm) of (a) **3** (dark yellow) and **7** (blue), and (b) **4** (dark yellow) and **8** (blue) in Ar-saturated benzonitrile at a delay time of 50 ps.

for **4** where the peak corresponding to the radical ion-pair were shadowed by intense peaks of parent donor entity. As shown in Fig. 10b, the spectrum recorded at 50 ps clearly showed cation radical peak at 610 nm and a shoulder peak of $C_{60}^{\cdot-}$ at 1020 nm. The k_{CS} and k_{CR} evaluated by monitoring rise and decay of the $C_{60}^{\cdot-}$ (see Fig. 9d inset) were found to be $4.1 \times 10^{10} \text{ s}^{-1}$ and $3.3 \times 10^8 \text{ s}^{-1}$, respectively. However, a major part of decay signal (biexponential) persisted beyond 3 ns time window of our instrument setup revealing charge stabilization.

The energy level diagram shown in Fig. 7 predicted formation of $^3C_{60}^*$ in the case of **1** and $^3BODIPY^*$ in the case of **2-4** conjugates during the process of charge recombination due high energy of the radical ion-pairs compared to the triplet energy of sensitizers. It is known that directly excited BODIPY derivatives do not populate the triplet excited states with high quantum efficiency via intersystem crossing.²⁹ This seems to be also true in the case of bis-styryl BODIPY derivatives where weak transient bands were observed. However, if charge recombination could populate the $^3BODIPY^*$ as in the case of **2-4**, then one could expect well developed transient peaks of $^3BODIPY^*$. Nanosecond transient absorption studies were performed to unravel such recombination path of the radical ion-pairs.

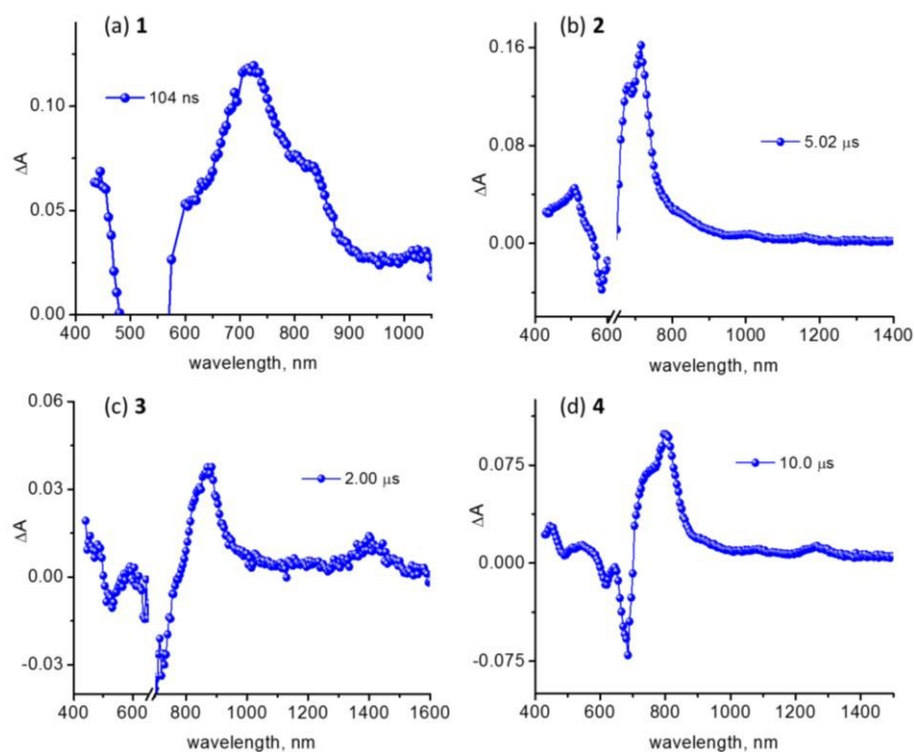


Fig. 11. Nanosecond transient spectrum at the indicated delay time of (a) **1** (505 excitation), (b) **2** (630 nm excitation), (c) **3** (685 nm excitation), and (d) **4** (355 nm excitation) in Ar-saturated benzonitrile.

Fig. 11 illustrates the nanosecond transient spectra of the donor-acceptor systems, **1-4** in benzonitrile. For **1**, the transient spectrum revealed a strong band at 700 nm and a shoulder band at 824 nm, characteristic of $^3\text{C}_{60}^*$ formation (Fig. 11a).³⁰ This indicates that the radical ion-pair populates the $^3\text{C}_{60}^*$, as predicted for **1** in Fig. 6, prior returning to the ground state. The $^3\text{C}_{60}^*$ thus formed relaxed to the ground state at a rate constant of $3.2 \times 10^5 \text{ s}^{-1}$. Well-defined transient spectra revealing peaks of $^3\text{BODIPY}^*$ (compared to their respective pristine $^3\text{BODIPY}^*$) and not that of $^3\text{C}_{60}^*$ were observed in the case of **2-4**. For **2**, the peak positions were close to that reported in literature for bis styryl BODIPY derivatives (Fig. 11b)^{21h,22} and appeared at 511 and 713 nm. The $^3\text{BODIPY}^*$ thus formed relaxed to the ground state at a rate constant of $2.5 \times 10^4 \text{ s}^{-1}$. For **3** and **4**, the transient peaks were red-shifted (Fig. 11c and 11d). For **3**, the transient peaks were at 590, 870 and 1408 nm which decayed at a rate constant of $4.2 \times 10^4 \text{ s}^{-1}$. Transient peaks of **4** were located at 450, 543, 801 and 1264 nm which decayed at a rate constant of $3.5 \times 10^3 \text{ s}^{-1}$.

A comparison between the presently investigated bis(donor styryl)BODIPY- C_{60} conjugates to the earlier reported BODIPY- C_{60} type dyads and triads was made. First, in the case of self-assembled bis(donor styryl)BODIPY- C_{60} conjugates (C_{60} was assembled via alkyl cation-crown ether complexation)²² having similar secondary electron donors, although the values of k_{CS} were close to that observed in the present study, the k_{CR} values were slightly lower due to the increased distance between BODIPY and C_{60} entities. In the case of donor-BODIPY- C_{60} triads in which the secondary donor and acceptor were directly attached to the BODIPY, as a result of close proximity between the entities, ultrafast charge separation and charge recombination was observed.^{24a,31a} Recently, a pyrrolyl-bridged BODIPY- C_{60} was reported by us.^{31c} Due to α -carbon substitution and extended conjugation offered by the pyrrole ring, efficient charge separation and recombination was observed. These studies bring out the importance of geometry and electronic structure of donor-acceptor systems in governing the kinetics of charge separation and charge recombination processes.

3. Summary

The multi-modular donor-acceptor systems built using bis-styryl BODIPY as the central unit and C_{60} and secondary electron donors revealed several interesting features. First, as a result of extended p-conjugation and strong electronic interactions between the secondary donors and styryl BODIPY π -system, these systems offered better spectral capture covering the visible and

near-infrared portions of the electromagnetic spectrum. Electrochemical studies helped in evaluating redox potentials of different entities of the multi-modular systems. The established energy level diagram, using spectral, electrochemical and computational results, helped in visualizing the mechanistic details of photophysical processes. Femtosecond transient absorbance studies provided evidence for the occurrence of charge separation in these donor-acceptor systems. Ultrafast charge separation and relatively slow charge recombination were witnessed. The charge recombination populated the $^3\text{C}_{60}^*$ in the case of donor-acceptor system lacking styryl groups, **1** while $^3\text{BODIPY}^*$ was formed in the case of systems having bis-styryl entities, **2-4** as evidenced by nanosecond transient absorption studies. The charge separation processes witnessed in these systems brought out their importance as broad band capturing, energy harvesting materials for solar energy harvesting and optoelectronic device building applications.

4. Experimental Section

4.1 Chemicals. Buckminsterfullerene, C_{60} (+99.95%) was from SES Research, (Houston, TX). All the reagents were from Aldrich Chemicals (Milwaukee, WI) while the bulk solvents utilized in the syntheses were from Fischer Chemicals. Tetra-*n*-butylammonium perchlorate, (*n*- Bu_4N) ClO_4 , used in electrochemical studies was from Fluka Chemicals. Synthetic details of control compounds, **5-8** is given in the ESI.

4.2 Syntheses

Synthesis of 1a: The aryl-difluoroboron dipyrin compounds were synthesized according to the procedure of Imahori and coworkers.³² To a mixture of methyl 4-formylbenzoate (12.4 mmol) and 2, 4-dimethylpyrrole (2.16 mL, 21.1 mmol) in 800 mL of dry dichloromethane, trifluoroacetic acid (0.19 mL, 2.47 mmol) was added. The reaction mixture was stirred for 2 hours at room temperature under nitrogen. After which the solution mixture was washed with 0.1M NaOH (200 mL) followed by water (200 mL). The organic layer was dried over anhydrous Na_2SO_4 and evaporated under reduced pressure. The residue was dissolved in toluene (50 mL) and *p*-chloranil (2.73 g, 11.1 mmol) was added. After 10 minutes, Et_3N (8 mL) was added followed by $\text{BF}_3 \cdot \text{Et}_2\text{O}$ (7 mL) and the mixture was stirred for 3 hours. To quench the reaction, the mixture was poured into water. The organic layer was extracted and dried over anhydrous

Na₂SO₄ and evaporated under reduced pressure. The crude product was purified using column chromatography using mixtures of CH₂Cl₂ and hexane as eluent.

Yield: 10.50 %. (¹H NMR in CDCl₃, 400 MHz, 25 °C), δ (ppm): 8.19 (d, 2 H, Ar-H), 7.41 (d, 2 H, Ar-H), 6.00 (s, 2H, pyrrole-H), 3.98 (s, 3 H, OCH₃-H), 2.57 (s, 6 H, CH₃-H), 1.37 (s, 6 H, CH₃-H).

Synthesis of 2b. Knoevenagel condensation reaction for the synthesis of bis(styryl)BODIPY compounds was accomplished according to the procedure of Rurack et. al.³³ BODIPY, **1a** (0.102 g, 0.268 mmoles) and benzaldehyde (0.134 g, 1.07 mmoles), piperidine (0.27 mL), and AcOH (0.17 mL) in benzene (15 mL) were refluxed and a reaction monitored using UV. Using Dean–Stark apparatus, the water formed during the reaction was removed azeotropically. When all the starting material had been consumed, the mixture was cooled to room temperature and washed with water. The organic phase was dried over Na₂SO₄ and solvent was evaporated under reduced pressure. The residue was purified by silica gel column chromatography with CH₂Cl₂/ hexane (2/3) eluting solvent system to afford the desired the compound **2b**.

Yield (3.2 %). ¹H NMR in CDCl₃, 400 MHz, 25 °C, δ (ppm):), 8.12-8.16 (d,2H, Ar-H), 7.66–7.70 (d,2 H, Ar-H,) 7.56–7.60 (d, 2H, Ar-H), 7.42–7.46 (m, 2 H, Ar-H), 7.32–7.38 (t, 4 H,Ar-H), 7.24–7.29 (m,2 H, Ar-H), 6.90-7.21 (m 4H) 6.60 (s, 2 H, pyrrole-H), 3.9 (s, 3H, H-OCH₃), 1.40 (s, 6 H, CH₃-H)

Synthesis of 3b. In a similar manner as **2b**, compound **3b** was synthesized, BODIPY **1a** (0.30 g, 0.78 mmoles) and diphenyl amino benzaldehyde(0.856 g, 3.13 mmoles) in a mixture of benzene (15 mL), piperidine (0.1 mL) and acetic acid (0.1 mL) were refluxed and reaction monitored by UV. The crude obtained by the reaction was purified on silica gel column using solvent system hexane and methylene chloride (1/1) to obtain the desired compound:

Yield (81.9%)UV/Vis ¹H NMR in CDCl₃, 400 MHz, 25 °C:¹H NMR (400 MHz, CDCl₃) δ = 8.16 (d, 2H, Ar-H), 7.58 (d,2H, Ar-H), 7.42-7.8 (m, 6H, Ar-H), 7.26-7.29 (m, 8H, Ar-H), 7.16 (d, 2H, Ar-H), 7.08-7.15 (m, 8H-Ar-H), 7.00-7.08 (m, 8H), 6.56(s, 2H), 3.59 (s, 3H), 1.50(s, 6H)

Synthesis of 4b. Compound **1a** (0.037g,0.09 mmoles) and 3-formyl-10-methyl-4aH-phenothiazin-10-ium (0.064 g, 0.261 mmoles) in a mixture of benzene (15 mL), piperidine (0.1 mL) and acetic acid (0.1 mL) were refluxed and reaction monitored by UV-vis. The crude

obtained by the reaction was purified on silica gel column using solvent system hexane and methylene chloride (1/1) to obtain the desired compound:

Yield (21.5%). ^1H NMR in CDCl_3 , 400 MHz, 25 °C: δ = 8.10 (d, 2H) 7.50–7.56 ppm (d, 2 H Ar-H), 7.36–7.44 (m, 6 H, Ar-H), 7.34 (d, 2 H, Ar-H), 7.06–7.14 (m, 4H, Ar-H) 6.88–6.92 (m, 2H, Ar-H), 6.76–6.83 (m, 4 H), 6.54 (s, 2 H, pyrrole-H), 3.85 (s, 3H, $-\text{OCH}_3$ -H) 3.38 (s, 6 H, CH_3 -H), 1.50 (s, 6 H, CH_3 -H).

Synthesis of 2c. The ester on bis(styryl)BODIPY were hydrolyzed according to a procedure reported by Rampazzo and coworkers.³⁴ In a round-bottomed flask, compound **2b** (0.149 g, 0.264 mmoles) were dissolved in 2.5 mL of THF. To this solution, lithium hydroxide monohydrate (0.066 g, 1.322 mmoles) dissolved in 1.0 mL of water were rapidly added drop wise. The reaction mixture was stirred for 5 hours at room temperature. The mixture was then diluted with a 0.1 M solution of hydrochloric acid and extracted with dichloromethane and the organic phases were dried on sodium sulfate and evaporated under reduced pressure. The resulting mixture was purified by means of flash chromatography on silica gel using a methylene chloride/hexane (98:2 %) to afford compounds **2c**.

Yield (45.5 %). ^1H NMR in CDCl_3 , 400 MHz, 25 °C), δ (ppm):), 8.12–8.16 (d, 2H, Ar-H), 7.66–7.70 (d, 2 H, Ar-H,) 7.56–7.60 (d, 2H, Ar-H), 7.42–7.46 (m, 5 H, Ar-H), 7.38–7.42 (d, 2 H, Ar-H), 7.32–7.37 (t, 4 H, Ar-H), 7.24–7.29 (m, 2 H, Ar-H), 6.60 (s, 2 H, pyrrole-H), 1.40 (s, 6 H, CH_3 -H)

Synthesis of 3c. In a round-bottomed flask, compound **3b** (0.140 g, 0.157 mmoles) were dissolved in 2.5 mL of THF. To this solution, lithium hydroxide monohydrate (0.033 g, 0.784 mmoles) dissolved in 1.0 mL of water were rapidly added drop wise. The reaction mixture was stirred for 5 hours at room temperature. The mixture was then diluted with a 0.1 M solution of hydrochloric acid and extracted with dichloromethane and the organic phases were dried on sodium sulfate and evaporated under reduced pressure. The resulting mixture was purified by means of flash chromatography on silica gel using a methylene chloride/hexane (98:2 %) to afford compounds **3c**.

Yield (29.0%). ^1H NMR (400 MHz, CDCl_3): δ = 8.26 (d, 2H, Ar-H), 7.60 (d, 2H, Ar-H), 7.44–7.52 (m, 6H, Ar-H), 7.28–7.32 (m, 5H, Ar-H), 7.2 (d, 2H, Ar-H), 7.12–7.16 (m, 8H, Ar-H), 7.05–7.1(m, 8H, Ar-H), 7.00–7.04 (m, 8H, Ar-H), 6.6(s, 2H) 1.50(s, 6H)

Synthesis of 4c. In a round-bottomed flask, compound **4b** (0.228 g, 0.0273 mmol) were dissolved in 2.5 mL of THF. To this solution, lithium hydroxide monohydrate (0.0136 g, 0.273 mmol) dissolved in 1.0 mL of water were rapidly added drop wise. The reaction mixture was stirred for 5 hours at room temperature. The mixture was then diluted with a 0.1 M solution of hydrochloric acid and extracted with dichloromethane and the organic phases were dried on sodium sulfate and evaporated under reduced pressure. The resulting mixture was purified by means of flash chromatography on silica gel using a methylene chloride/hexane (98:2 %) to afford compounds **4c**.

Yield (68.50%). ¹H NMR (400 MHz, CDCl₃): δ = 8.10 (d, 2H), 7.46–7.56 ppm (d, 2H, CH-H), 7.36–7.44 (m, 4H, Ar-H), 7.32 (d, 2H, Ar-H), 7.06–7.16 (m, 5H, Ar-H), 6.92–6.96 (m, 3H, Ar-H), 6.76–6.83 (m, 6H, Ar-H), 6.54 (s, 2H, pyrrole-H), 3.38 (s, 6H, CH₃-H), 1.50 (s, 6H, CH₃-H).

Synthesis of 2d. In a round-bottom flask, **2c** (0.034 g, 0.062 mmol) and 4-hydroxy benzaldehyde (0.038 g, 0.31 mmol) were dissolved dry methylene chloride (25 ml) to this, 4-dimethylaminopyridine, DMAP (0.038 g, 0.31 mmol) was added. The resulting solution was cooled to 0 °C, followed by addition of dicyclohexylcarbodiimide, DCC (0.064 g, 0.31 mmol). The reaction mixture was stirred under nitrogen for 6 hours at room temperature. Excess solvent was removed under vacuum and the crude compound was washed with water several times and extracted with CHCl₃. Purification of the crude compound was carried out on a silica gel column with hexane/ dichloromethane (1/4) as eluent giving the compound **2d**.

Yield (47.5 %). ¹H NMR in CDCl₃, 400 MHz, 25 °C, δ (ppm): 10.1 (s, 1H, CHO), 8.12–8.16 (d, 2H, Ar-H), 7.66–7.70 (d, 2H, Ar-H), 7.56–7.60 (d, 2H, Ar-H), 7.38–7.42 (d, 2H, Ar-H), 7.32–7.37 (t, 4H, Ar-H), 7.24–7.29 (m, 2H, Ar-H), 6.60 (s, 2H, pyrrole-H), 3.9 (s, 3H, H-OCH₃), 1.40 (s, 6H, CH₃-H)

Synthesis of 3d. In a round-bottom flask, **3c** (0.040 g, 0.045 mmol) and 4-hydroxy benzaldehyde (0.028 g, 0.22 mmol) were dissolved dry methylene chloride (25 mL). To this, DMAP (0.028 g, 0.220 mmol) was added. The resulting solution was cooled to 0 °C, followed by addition of DCC (0.046 g, 0.220 mmol). The reaction mixture was stirred under nitrogen for 6 hours at room temperature. Excess solvent was removed under vacuum and the crude compound was washed with water several times and extracted with dichloromethane.

Purification of the crude compound was carried out on a silica gel column with hexane/dichloromethane (1/4) as eluent giving the compound **3d**.

Yield (50.7 %). ^1H NMR (400 MHz, CDCl_3) δ = 10.0 (s, 1H), 8.26 (d, 2H), 7.90 (d, 2H), 7.44-7.52 (m, 10H), 7.28-7.32 (m, 6H), 7.2 (d, 2H), 7.12-7.16 (m, 10H), 7.00-7.1 (m, 9H), 6.6(s, 2H) 1.50(s, 6H)

Synthesis of 4d. In a round-bottom flask, **3d** (0.021 g, 0.026 mmoles) and 4-hydroxy benzaldehyde (0.0157 g, 0.129 mmoles) were dissolved dry methylene chloride (25 mL), and to this, DMAP (0.016 g, 0.129 mmoles) was added. The resulting solution was cooled to 0 °C, followed by addition of DCC (0.027 g, 0.129 mmoles). The reaction mixture was stirred under nitrogen for 6 hours at room temperature. Excess solvent was removed under vacuum and the crude compound was washed with water several times and extracted with dichloromethane. Purification of the crude compound was carried out on a silica gel column with hexane/dichloromethane (1/9) as eluent giving the compound **4d**.

Yield (87.2 %). ^1H NMR in CDCl_3 , 400 MHz, 25 °C), δ =10.05 (s, 1-CHO) 8.35 (d, 2H), 8.05 (d, 2H), 7.65 (d, 2H, Ar-H), 7.55 (d, 2H Ar-H), 7.50 (d, 4H, Ar-H) 7.45 (d, 2H Ar-H) 7.15–7.25 (m, 5 H, Ar-H), 7.32 (d, 2 H, Ar-H), 6.95–6.96 (m, 3 H, Ar-H), 6.85–6.90 (d, 2H, Ar-H), , 6.55 (s, 2 H, pyrrole-H), 3.45 (s, 6 H, CH_3 -H), 1.50 (s, 6 H, CH_3 -H).

Synthesis of 2. Using Prato's³⁵ method, compound **2** was synthesized as follows. To dry toluene (25 mL) in a round-bottomed flask, compound **2d** (0.0194 g, 0.0299 mmoles.), C_{60} (0.0645 g, 0.0896 mmoles), and sarcosine (0.0133 g, 0.149 mmoles) were refluxed for 12 hours. After cooling to room temperature, the solvent was evaporated and the crude was purified on silica by flash chromatography using toluene/hexane 9.5/0.5 v/v) solvent system affording the final compounds **2**.

Yield (60.3%). ^1H NMR (250 MHz, CDCl_3) δ = 8.30 (d, 2H), 7.64 (d, 2H) 7.58 (d, 4H), 7.50 (d, 2H), 7.26-7.38 (m, 10H), 6.90 (d, 2 H), 6.6 (s, 2), 5.0 (s, 2H), 4.25 (dd, 1H), 2.85 (s, 3H), 1.45 (s, 6H). MS (MALDI): Calcd, 1395.29 [M+]; found 1395.8. ^{13}C NMR (400 MHz, CDCl_3):163.41, 152.114, 149.81, 146.36, 145.68, 145.46, 145.35, 145.26, 145.15, 144.99, 144.78, 144.56, 144.47, 144.34, 144.27, 144.20, 143.74,143.45, 142.19, 142.04, 141.74, 141.27, 147.20, 141.13, 141.08, 140.80, 140.59, 139.84, 139.24, 138.95, 138.57, 135.75, 135.46, 129.88, 129.17, 128.16, 127.83, 126.64, 118.14, 117.17, 81.95, 76.28, 76.03, 75.76, 39.13, 30.95, 29.06, 28.72, 28.38, 21.71, 13.93.

Synthesis of 3. To dry toluene (20 mL) in a round-bottomed flask, compound **3d** (0.023 g, 0.0232 mmoles), C₆₀ (0.051 g, 0.0695 mmoles), and sarcosine (0.010g, 0.116 mmoles) were refluxed for 12 hours. After cooling to room temperature, the solvent was evaporated and the crude was purified on silica by flash chromatography using toluene/hexane 9.5/0.5 v/v) solvent system affording the final compounds **3**.

Yield (55.8%). ¹H NMR (400 MHz, CDCl₃) δ = 8.26 (d, 2H), 7.54 (d, 2H), 7.46 (d, 2H), 7.40 (d, 4H), 7.30 (d, 2H), 7.44-7.52 (m, 6H), 7.28-7.32 (m, 7H), 7.2 (d, 2H), 7.12-7.16 (m, 9H), 7.00-7.1 (m, 8H), 6.6 (s, 2H), 4.95 (d, 2H, fulleropyrrolidine-H), 4.45 (d, 1H, fulleropyrrolidine-H), 1.50 (s, 6H). ¹³C NMR (250 MHz, CDCl₃): 148.7, 147.3, 147.1, 146.6, 146.3, 146.2, 146.1, 146.9, 146.5, 145.3, 145.2, 145.1, 144.7, 144.6, 144.3, 142.7, 142.6, 142.2, 142.1, 141.6, 140.2, 139.9, 135.9, 130.7, 130.2, 129.4, 128.6, 126.3, 125.1, 123.0, 122.4, 82.9, 77.3, 77.0, 76.7, 75.5, 70.0, 69.5, 40.1, 29.7, 14.8. MS (MALDI): Calcd, 1729.29 [M⁺]; found 1729.6.

Synthesis of 4. To dry toluene (20 mL) in a round-bottomed flask, compound **4d** (0.021 g, 0.0266 mmoles.), C₆₀ (0.0575 g, 0.0798 mmoles), and sarcosine (0.119 g, 0.133 mmoles) were refluxed for 12 hours. After cooling to room temperature, the solvent was evaporated and the crude was purified on silica by flash chromatography using toluene solvent system affording the final compounds **4**.

Yield (63.3%). ¹H NMR in CDCl₃, 400 MHz, 25 °C), δ = 8.35 (d, 2H), 8.10 (d, 2H), 7.88- 8.0 (m, 4 H, Ar-H), 7.65 (d, 2 H, Ar-H), 7.41-7.50 (, 6H, Ar-H), 7.32-7.40 (m, 8 H, Ar-H), 6.85- 6.90 (d, 2H, Ar-H), 6.55 (s, 2 H, pyrrole-H), 5.0 (d, 2H, fulleropyrrolidine-H), 4.42 (d, 1H, fulleropyrrolidine-H), 3.49 (s, 6 H, CH₃-H), 2.87 (s, 3H, CH₃-H), 1.50 (s, 6 H, CH₃-H).), MS (MALDI): Calcd, 1665.32 [M⁺]; found 1665.2.

4.3 Spectral measurements

The UV-visible spectral measurements were carried out with a Shimadzu Model 2550 double monochromator UV-visible spectrophotometer. The fluorescence emission was monitored by using a Varian Eclipse spectrometer. A right angle detection method was used. The ¹H NMR studies were carried out on a Varian 400 MHz spectrometer. Tetramethylsilane (TMS) was used as an internal standard. Differential pulse voltammograms were recorded on an EG&G PARSTAT electrochemical analyzer using a three electrode system. A platinum button electrode was used as the working electrode. A platinum wire served as the counter electrode and an

Ag/AgCl electrode was used as the reference electrode. Ferrocene/ferrocenium redox couple was used as an internal standard. All the solutions were purged prior to electrochemical and spectral measurements using nitrogen gas.

4.4 Femtosecond pump-probe transient spectroscopy. Femtosecond transient absorption spectroscopy experiments were performed using an Ultrafast Femtosecond Laser Source (Libra) by Coherent incorporating diode-pumped, mode locked Ti:Sapphire laser (Vitesse) and diode-pumped intra cavity doubled Nd:YLF laser (Evolution) to generate a compressed laser output of 1.45 W. For optical detection, a Helios transient absorption spectrometer coupled with femtosecond harmonics generator both provided by Ultrafast Systems LLC was used. The source for the pump and probe pulses were derived from the fundamental output of Libra (Compressed output 1.45 W, pulse width 100 fs) at a repetition rate of 1 kHz. 95% of the fundamental output of the laser was introduced into harmonic generator which produces second and third harmonics of 400 and 267 nm besides the fundamental 800 nm for excitation, while the rest of the output was used for generation of white light continuum. In the present study, the second harmonic 400 nm excitation pump was used in all the experiments. Kinetic traces at appropriate wavelengths were assembled from the time-resolved spectral data. Data analysis was performed using Surface Explorer software supplied by Ultrafast Systems. All measurements were conducted in degassed solutions at 298 K. The estimated error in the reported rate constants is $\pm 10\%$.

4.5 Nanosecond laser flash photolysis. The studied compounds were excited by a Opolette HE 355 LD pumped by a high energy Nd:YAG laser with second and third harmonics OPO (tuning range 410-2200 nm, pulse repetition rate 20 Hz, pulse length 7 ns) with the powers of 1.0 to 3 mJ per pulse. The transient absorption measurements were performed using a Proteus UV-Vis-NIR flash photolysis spectrometer (Ultrafast Systems, Sarasota, FL) with a fibre optic delivered white probe light and either a fast rise Si photodiode detector covering the 200-1000 nm range or a InGaAs photodiode detector covering 900-1600 nm range. The output from the photodiodes and a photomultiplier tube was recorded with a digitizing Tektronix oscilloscope.

Acknowledgments

Support by the National Science Foundation (Grant No. 1401188) is acknowledged. The computational work was performed at the Holland Computing Centre of the University of Nebraska.

Notes and references

‡ Crystallographic data have been deposited with the Cambridge Crystallographic Data Centre with CCDC reference number CCDC 1480541 (for **6**). Copies of the data can be obtained, free of charge, on application to CCDC, 12 Union Road, Cambridge CB2 1EZ, UK <http://www.ccdc.cam.ac.uk/perl/catreq/catreq.cgi>, e-mail: data_request@ccdc.cam.ac.uk, or fax: +44 1223 336033.

Electronic Supplementary Information (ESI) available: [structure, absorption spectra and synthesis of control compounds **5-8**, spectra of oxidized probes, X-ray structural details of **6**, ^1H , ^{13}C and MALDI-mass spectra of newly synthesized compounds]. See DOI: 10.1039/x0xx00000x

References

1. a) S. D. Straight, G. Kodis, Y. Terazono, M. Hambourger, T. A. Moore, A. L. Moore and D. Gust, *Nature Nanotechnol.*, 2008, **3**, 280; (b) D. Gust, T. A. Moore and A. L. Moore, *Acc. Chem. Res.*, 2009, **42**, 1890; (c) D. Gust, T. A. Moore and A. L. Moore, *Faraday Discuss.*, 2012, **155**, 9.
2. M. R. Wasielewski, *Acc. Chem. Res.*, 2009, **42**, 1910.
3. a) D. M. Guldi, A. Rahman, V. Sgobba and C. Ehli, *Chem. Soc. Rev.*, 2006, **35**, 471; (b) J. N. Clifford, G. Accorsi, F. Cardinali, J. F. Nierengarten and N. Armaroli, *C. R. Chimie.*, 2006, **9**, 1005; (c) N. Martin, L. Sanchez, M. A. Herranz, B. Illesca and D. M. Guldi, *Acc. Chem. Res.*, 2007, **40**, 1015; (d) G. Bottari, G. de la Torre and D. M. Guldi, T. Torres, *Chem. Rev.*, 2010, **110**, 6768; (f) D. M. Guldi and V. Sgobba *Chem. Commun.*, 2011, **47**, 606; (g) D. Gonzalez-Rodriguez, E. Carbonell and D. M. Guldi, *Angew. Chem. Int. Ed.*, 2009, **48**, 8032.
4. a) E. M. Pérez and N. Martín, *Chem. Soc. Rev.*, 2008, **37**, 1512; (b) K. Dirian, M. A. Herranz, G. Katsukis, J. Malig, L. Rodriguez-Perez, D. Romero-Nieto, V. Strauss, N. Martin and D. M. Guldi, *Chem. Sci.*, 2013, **4**, 4335; (c) L. Sanchez, N. Martin and D. M. Guldi, *Angew. Chem., Int. Ed.*, 2005, **44**, 5374.
5. J. S. Lindsey and D. F. Bocian, *Acc. Chem. Res.*, 2011, **44**, 638-650.
6. a) S. Fukuzumi, *Phys. Chem. Chem. Phys.*, 2008, **10**, 2283; (b) S. Fukuzumi and T. Kojima, *J. Mater. Chem.*, 2008, **18**, 1427; (c) S. Fukuzumi, T. Honda, K. Ohkubo and T. Kojima, *Dalton Trans.*, 2009, 3880; (d) S. Fukuzumi and K. Ohkubo, *J. Mater. Chem.*,

- 2012, **22**, 4575. (e) S. Fukuzumi, K. Ohkubo and T. Suenobu, *Acc. Chem. Res.*, 2014, **47**, 1455-1464.
7. a) M. E. El-Khouly, O. Ito, P. M. Smith and F. D'Souza, *J. Photochem. Photobiol. C.*, 2004, **5**, 79; (b) F. D'Souza and O. Ito, *Coord. Chem. Rev.*, 2005, **249**, 1410; (c) F. D'Souza and O. Ito, *Chem. Commun.*, 2009, 4913; (d) F. D'Souza, A. S. D. Sandanayaka and O. Ito, *J. Phys. Chem. Letts.*, 2010, **1**, 2586; (e) F. D'Souza and O. Ito, *Chem. Soc. Rev.*, 2012, **41**, 86; (f) F. D'Souza and O. Ito, In *Multiporphyrin Array: Fundamentals and Applications*, (Ed. D. Kim), Pan Stanford Publishing: Singapore, 2012, Chapter 8, pp 389. (g) C. B. KC and F. D'Souza, *Coord. Chem. Rev.*, 2016, in press. <http://dx.doi.org/doi:10.1016/j.ccr.2016.05.012>.
8. a) J. L. Sessler, C. M. Lawrence and J. Jayawickramarajah, *Chem. Soc. Rev.*, 2007, **36**, 314; (b) S. Fukuzumi, K. Ohkubo, F. D'Souza and J. L. Sessler, *Chem. Commun.*, 2012, **48**, 9801.
9. a) R. Ziessel and A. Harriman, *Chem. Commun.*, **2011**, 47, 611; (b) A. C. Benniston and A. Harriman, *Coord. Chem. Rev.*, 2008, **252**, 2528.
10. a) G. Ulrich, R. Ziessel and A. Harriman, *Angew. Chem. Int. Ed.*, 2008, **47**, 1184; (b) M. El-Khouly, S. Fukuzumi and F. D'Souza, *ChemPhysChem*, 2014, **15**, 30; (c) C. B. KC and F. D'Souza, *Coord. Chem. Rev.*, 2016, in press, [doi:10.1016/j.ccr.2016.05.012](http://dx.doi.org/doi:10.1016/j.ccr.2016.05.012).
11. a) *Organic Nanomaterials* Eds. T. Torres and G. Bottari, Wiley-VCH, Weinheim, 2013, pp 187; (b) O. Ito and F. D'Souza in *From Molecules to Materials: Pathways to Artificial Photosynthesis*, Eds. E. A. Rozhkova, K. Ariga, Springer, Switzerland, 2015.
12. A. Satake and Y. Kobuke, *Org. Biomol. Chem.*, 2007, **5**, 1679.
13. a) *Energy Harvesting Materials* (Ed.: D. L. Andrews), World Scientific, Singapore. 2005; (b) S. Gunes, H. Neugebauer and N. S. Sariciftci, *Chem. Rev.*, 2007, **107**, 1324.
14. a) N. Armaroli and V. Balzani, *Angew. Chem.*, 2007, **119**, 52; (b) N. Armaroli and V. Balzani, *Angew. Chem. Int. Ed.*, 2007, **46**, 52; (c) V. Balzani, A. Credi and M. Venturi, *ChemSusChem*, 2008, **1**, 26.
15. a) H. Imahori, T. Umeyama and S. Ito, *Acc. Chem. Res.*, 2009, **42**, 1809-1818. b) T. Umeyama and H. Imahori, *Energy Environ. Sci.*, 2008, **1**, 120.
16. T. Hasobe, *Phys. Chem. Chem. Phys.*, 2010, **12**, 44-57.

17. a) N. S. Lewis and D. G. Nocera, *Proc. Natl. Acad. Sci. U. S. A.*, 2006, **103**, 15729; (b) D. G. Nocera, *Inorg. Chem.*, 2009, **48**, 10001.
18. P. V. Kamat, *J. Phys. Chem. C*, 2007, **111**, 2834.
19. a) I. Obraztsov, W. Kutner and F. D'Souza in *Electrochemistry of N4 Macrocyclic Complexes*, Eds, J. H. Zagal and F. Bedioui, Springer, 2016, pp 171; (b) K. H. Joya, Y. F. Joya, K. Ocakoglu and R. van de Krol, *Angew. Chem. Int. Ed.*, 2013, **52**, 10426; (c) Y. Tachibana, L. Vayssieres and J. R. Durrant, *Nature Photonics*, 2012, **6**, 511; (d) D. Gust and T. A. Moore, *Science*, 1989, **244**, 35.
20. a) A. C. Benniston and G. Copley, *Phys. Chem. Chem. Phys.*, 2009, **11**, 4124; (b) H. N. Kim, W. X. Ren, J. S. Kim and J. Yoon, *Chem. Soc. Rev.*, 2012, **41**, 3210 (c) Y. Ni, J. W. *Org. Biomol. Chem.*, 2014, **12**, 3774.
21. For covalently linked styrylBODIPY donor-acceptor see: a) J.-Y. Liu, M. E. El-Khouly, S. Fukuzumi and D. K. P. Ng, *Chem. Eur. J.*, 2011, **6**, 174; (b) J.-Y. Liu, E. A. Ermilov, B. Roder and D. K. P. Ng, *Chem. Commun.*, 2009, 1517; (c) L. Huang, X. Yu, W. Wu and J. Zhao, *Org. Letts.* 2012, **14**, 2594; (d) Z. Kostereli, T. Ozdemir, O. Buyukcakir and E. U. Akkaya, *Org. Letts.*, 2012, **14**, 3636; (e) A. Nano, R. Ziessel, P. Stachelek and A. Harriman, *Chem. Eur. J.*, 2013, **19**, 13528; (f) L. Haung, X. Cui, B. Therrien and J. Zhao, *Chem. Eur. J.*, 2013, **19**, 17472; (g) M. Di Donato, A. Iagatti, A. Lapini, P. Foggi, S. Cicchi, L. Lascialfari, S. Fedeli, S. Caprasecca and B. Mennuci, *J. Phys. Chem. C*, 2014, **118**, 23476. h) S. Guo, L. Xu, K. Xu, J. Zhao, B. Kucukoz, A. Karatay, H. G. Yaglioglu, M. Hayvali, A. Elmali, *Chem. Sci.*, 2015, **6**, 3724.
22. S. Shao, H. B. Gobeze, P. A. Karr and F. D'Souza, *Chem. Eur. J.*, 2015, **21**, 16005.
23. See ESI for structural details.
24. a) C. B. KC, G. N. Lim, V. N. Nesterov, P. A. Karr and F. D'Souza. *Chem. Eur. J.*, 2014, **20**, 17100; (b) J. H. Gibbs, Z. Zhou, D. Kessel, F. R. Fronczek, S. Pakhomova and M. G. H. Vicente, *J. Photochem. Photobiol. B Biology*, 2015, **145**, 35.
25. J. R. Lakowicz, *Principles of Fluorescence Spectroscopy*, 3rd ed., Springer, Singapore, 2006.
26. *Gaussian 09*, M. J. Frisch, G. W. Trucks, H. B. Schlegel, G. E. Scuseria, M. A. Robb, J. R. Cheeseman, V. G. Zakrzewski, J. A. Montgomery, R. E. Stratmann, J. C. Burant, S. Dapprich, J. M. Millam, A. D. Daniels, K. N. Kudin, M. C. Strain, O. Farkas, J. Tomasi,

- V. Barone, M. Cossi, R. Cammi, B. Mennucci, C. Pomelli, C. Adamo, S. Clifford, J. Ochterski, G. A. Petersson, P. Y. Ayala, Q. Cui, K. Morokuma, D. K. Malick, A. D. Rabuck, K. Raghavachari, J. B. Foresman, J. Cioslowski, J. V. Ortiz, B. B. Stefanov, G. Liu, A. Liashenko, P. Piskorz, I. Komaromi, R. Gomperts, R. L. Martin, D. J. Fox, T. Keith, M. A. Al-Laham, C. Y. Peng, A. Nanayakkara, C. Gonzalez, M. Challacombe, P. M. W. Gill, B. G. Johnson, W. Chen, M. W. Wong, J. L. Andres, M. Head-Gordon, E. S. Replogle and J. A. Pople, Gaussian, Inc., Pittsburgh PA, 2009.
27. C. A. Wijesinghe, M. E. El-Khouly, N. K. Subbaiyan, M. Supur, M. E. Zandler, K. Ohkubo, S. Fukuzumi and F. D'Souza *Chem. Eur. J.*, 2011, **17**, 3147.
28. D. Rehm and A. Weller, *Isr. J. Chem.*, 1970, **8**, 259.
29. a) A. Loudet and K. Burgess, *Chem. Rev.*, 2007, **107**, 4891; (b) N. Boens, V. Leen and W. Dehaen, *Chem. Soc. Rev.*, 2012, **41**, 1130; (c) J. Suk, K. M. Omer, T. Bura, R. Ziessel and A. J. Bard, *J. Phys. Chem. C*, 2011, **115**, 15361.
30. D. M. Guldi and P. V. Kamat in *Fullerenes* Eds.: K. M. Kadish and R. S. Ruoff, Wiley, New York, 2000, Chapter 5, pp 225.
31. a) C. A. Wijesinghe, M. E. El-Khouly, J. D. Blakemore, M. E. Zandler, S. Fukuzumi and F. D'Souza, *Chem. Commun.*, 2010, **46**, 3301. b) V. Bandi, H. B. Gobeze and F. D'Souza, *Chem. Eur. J.*, 2015, **21**, 11483. c) V. Bandi, H. B. Gobeze, V. Lakshmi, M. Ravikanth and F. D'Souza, *J. Phys. Chem. C*, 2015, **119**, 8095.
32. C. Luo, D. M. Guldi, H Imahori, K. Tamaki and Y. Sakata, *J. Am. Chem. Soc.*, 2000, **122**, 6535.
33. K. Rurack, M. Kollmannsberger and J Daub, *Angew. Chem., Int. Ed.*, 2001, **40**, 385.
34. E. Rampazzo, S. Bonacchi, D. Genovese, R. Juris, M. Montalti, V. Paterlini, N. Zaccheroni, C. Dumas-Verdes, G. Clavier and R. Meallet-Renault, *J. Phys. Chem. C*, 2014, **118**, 9261.
35. M. Maggini, G. Scorrano and M. Prato, *J. Am. Chem. Soc.*, 1993, **115**, 9798.

Table of Contents

